Mathematical and Computer Modelling 55 (2012) 2029–2039

Contents lists available at SciVerse ScienceDirect

Mathematical and Computer Modelling

journal homepage: www.elsevier.com/locate/mcm

A quantitative ultrasound model of the bone with blood as the interstitial fluid☆

Robert P. Gilbert*, Philippe Guyenne, M. Yvonne Ou

Department of Mathematical Sciences, University of Delaware, Newark, DE 19716, USA

ARTICLE INFO

Article history:
Received 28 September 2011
Received in revised form 30 November 2011
Accepted 2 December 2011

Keywords:
Shear-thinning pore fluid
Ultrasound
Poroelasticity

ABSTRACT

A variant of the Biot–Johnson model of a poroelastic material is investigated to see if the viscosity of the interstitial fluid is significant in the ultrasound insonification of non-defatted cancellous bone. The equations of motion are derived using a Lagrangian formulation. Numerical experiments are performed on various bone samples. It is shown that the viscosity of the interstitial fluid does indeed signify in the ultrasound frequency range.

1. Introduction

As the brittleness of bone depends on more factors than bone density, biologists believe that quantitative ultrasound techniques could provide an important new diagnostic tool [1–5]. In this paper, we use the Biot theory [6,7] of a poroelastic material to investigate whether this is possible. The Biot theory which is obtained from mixture theory can only be applied in the low frequency range ($<$100 kHz), which corresponds to wave lengths sufficiently larger than the pore size. The Biot theory predicts a fast and slow compressional wave. The second compressional wave does not exist for elastic materials, so the detection of two different compressional waves signifies the poroelastic property of a specimen. Hosokawa and Otani [8] (see also [9]) identified fast and slow waves in cancellous bone. Cancellous bone consists of solid matrix and blood–marrow mixture, which acts like a non Newtonian shear thinning fluid [10–12] and is better modeled as complex polymers. However, the role played by bone marrow in ultrasound measurement for bone is still under debate. Some researchers [13,14] claim that taking into account marrow viscosity leads only to minor differences on the effective attenuation and dispersion. Nicholson and Bouxsein [15] made quantitative ultrasound (QUS) transmission and backscatter experiments on 46 human cancellous bone specimens where they considered both the water filled samples and the in vitro samples. They concluded that the potential impact of marrow should be considered when interpreting QUS measurement. In this paper, we study a modified form of the Biot–Johnson [16] equations to try and determine whether the interstitial fluid is a factor for interpreting the results of QUS. Indeed, there are two possibilities where the viscosity of a shear thinning material as the blood–marrow mixture could play a role. One is the fluid–fluid reaction of the interstitial fluid with itself, the other being the fluid–solid reaction of the blood–marrow with the trabeculae. It will turn out that for our model, only the latter effect is the dominant one. We have used a Carreau model to describe the blood–marrow mixture; however, it is primarily the viscosity of the mixture which signifies.

2. Constitutive equations for an isotropic, shear-thinning porous medium

The Biot model treats the medium as an elastic frame with interstitial pore fluid. Two displacement vectors

☆ This work was funded in part by the National Science Foundation Research Math. Biology Grants DMS-0920850 and 0920852.
* Corresponding author. Tel.: +1 302 368 3482.
E-mail addresses: gilbert@math.udel.edu (R.P. Gilbert), guyenne@math.udel.edu (P. Guyenne), mou@math.udel.edu (M. Yvonne Ou).

0895-7177/$ – see front matter © 2011 Elsevier Ltd. All rights reserved.
doi:10.1016/j.mcm.2011.12.004

$$\mathbf{u}(\mathbf{x}, t) = \langle u(\mathbf{x}, t), v(\mathbf{x}, t), w(\mathbf{x}, t)\rangle,$$

and

$$\mathbf{U}(\mathbf{x}, t) = \langle U(\mathbf{x}, t), V(\mathbf{x}, t), W(\mathbf{x}, t)\rangle, \tag{2.1}$$

with $\mathbf{x} := \langle x, y, z\rangle$ track the motion of the frame and fluid respectively while the divergences $e = \nabla \cdot \mathbf{u}$ and $\epsilon = \nabla \cdot \mathbf{U}$ give the frame and fluid dilatations. We denote the strain tensors as $\underline{e}$ and $\underline{\epsilon}$. Their six components are denoted by

$$e_{xx} = \frac{\partial u}{\partial x}, \qquad e_{yy} = \frac{\partial v}{\partial y}, \qquad e_{zz} = \frac{\partial w}{\partial z},$$
$$e_{xy} = \frac{1}{2}\left(\frac{\partial u}{\partial y} + \frac{\partial v}{\partial x}\right), \qquad e_{xz} = \frac{1}{2}\left(\frac{\partial u}{\partial z} + \frac{\partial w}{\partial x}\right), \qquad e_{yz} = \frac{1}{2}\left(\frac{\partial w}{\partial y} + \frac{\partial v}{\partial z}\right).$$

The corresponding stresses will be denoted by

$$\sigma_{xx}, \sigma_{yy}, \sigma_{zz}, \sigma_{xy}, \sigma_{xz}, \sigma_{yz},$$

and these expressions will depend on the constitutive relations. We shall treat only the case of an isotropic frame. In the Biot model the fluid stress in the pore space is given by $\sigma(\mathbf{x}, t) = -\beta p_f$, where p_f is the pressure of the pore fluid and the parameter β is the fraction of fluid area per unit cross section. Biot makes the assumption of statistical isotropy, that is, that β is the same for all cross sections. Thus β is equal to the porosity of the medium (volume of the pore space per unit volume).

In an isotropic medium the strain energy will be a function

$$W = W(I_1, I_2, I_3, \epsilon),$$

where the I_j are the three elastic invariants (see [17])

$$I_1 = e_{xx} + e_{yy} + e_{zz} = e,$$
$$I_2 = e_{yy}e_{zz} + e_{xx}e_{zz} + e_{xx}e_{yy} - \frac{1}{4}\left(e_{yz}^2 + e_{xz}^2 + e_{xy}^2\right),$$
$$I_3 = e_{xx}e_{yy}e_{zz} + \frac{1}{4}\left(e_{yz}e_{xz}e_{xy} - e_{xx}e_{yz}^2 - e_{yy}e_{xz}^2 - e_{zz}e_{xy}^2\right).$$

For small amplitude vibrations we can neglect powers of the displacements above the first order and obtain linear constitutive equations. This corresponds to a strain energy function that is purely quadratic in the strains and hence it will be a linear combination of the four quadratic terms [18–20] e^2, I_2, $e\epsilon$ and ϵ^2:

$$W = \frac{P}{2}e^2 - 2\mu I_2 + Qe\epsilon + \frac{R}{2}\epsilon^2.$$

From this we are able to obtain the Biot constitutive equations

$$\sigma_{xx} = \lambda e + 2\mu e_{xx} + Q\epsilon,$$
$$\sigma_{yy} = \lambda e + 2\mu e_{yy} + Q\epsilon,$$
$$\sigma_{zz} = \lambda e + 2\mu e_{zz} + Q\epsilon,$$
$$\sigma_{xy} = 2\mu e_{xy}, \qquad \sigma_{xz} = 2\mu e_{xz}, \qquad \sigma_{yz} = 2\mu e_{yz},$$
$$\sigma = Qe + R\epsilon, \tag{2.2}$$

where λ and μ are Lamé coefficients with $\lambda := P - 2\mu$. The symbols assigned to the parameters λ and μ are due to their formal analogy to the Lamé coefficients in the constitutive equations of an elastic solid. Indeed the tangential stress equations suggest that μ is the Lamé coefficient of shear for the frame, however as we shall see, λ is not the frame compressional coefficient.

In the Biot theory there is only dissipation of energy between the fluid and solid phases due to friction. We wish to generalize this theory to cover the case where there can be fluid to fluid dissipation also. To this end we consider the problem using a Lagrangian formulation. Let K represent the kinetic energy of the system, then we follow Biot [18] and express this as

$$K\left(\dot{\mathbf{u}}, \dot{\mathbf{U}}\right) = \frac{1}{2}\left[\rho_{11}\dot{\mathbf{u}}^2 + 2\rho_{12}\dot{\mathbf{u}} \cdot \dot{\mathbf{U}} + \rho_{22}\dot{\mathbf{U}}^2\right]. \tag{2.3}$$

The ρ_{11} and ρ_{22} are effective mass density parameters of the frame and fluid respectively and ρ_{12} is a mass coupling parameter for the frame–fluid interaction.

Biot [18,19] admits fluid–solid dissipation in the form of a dissipation force

$$b\left(\dot{\mathbf{u}} - \dot{\mathbf{U}}\right).$$

For the case of high frequency oscillations he notes that b is actually a function of ω. This really makes no sense mathematically but is useful for some computations. It would be better to replace the fluid to solid dissipation force by a convolution,

$$\mathbf{F}_{\text{fluid–solid}} = \int_0^t b(t-\tau)\left(\dot{\mathbf{u}}(\tau) - \dot{\mathbf{U}}(\tau)\right)\, d\tau. \tag{2.4}$$

The coupling between the fluid part (marrow) and elastic matrix (trabecular bone) is described by the Johnson–Koplik–Dashen model [16]. In this model, the dynamic tortuosity $\alpha(\omega)$ is expressed as a function of tortuosity α_∞, pore fluid viscosity η, pore fluid density ρ_f, permeability k, porosity β, the angular frequency ω and the viscous characteristic length Λ

$$\alpha(\omega) = \alpha_\infty\left(1 + \frac{\eta\beta}{i\omega\alpha_\infty\rho_f k}\sqrt{1 + i\frac{4\alpha_\infty^2 k^2\rho_f\omega}{\eta\Lambda^2\beta^2}}\right), \tag{2.5}$$

where $i = \sqrt{-1}$.

By comparing the Fourier transform of the Biot equations with the Johnson formulation we conclude that the Fourier transform of the friction coefficient between the solid and fluid phases, $\hat{b}(\omega)$, must be given by [21]

$$\hat{b}(\omega) = \frac{2\beta a_\infty}{\Lambda}\sqrt{i\rho_f\eta\omega},$$

and

$$b(t) := -\frac{1}{2\pi}\beta\alpha_\infty\sqrt{i\rho_f\eta}(t+0i)^{-\frac{3}{2}}\ \text{Heaviside}(t), \tag{2.6}$$

which is a distribution; moreover, the corresponding limit kernel $b(t)$ is not integrable. This suggests that an alternate form of the Johnson formula is better suited for describing the attenuation due to the friction of the fluid–solid interaction. One possibility is to use a transformed $b(t)$ which agrees with the Johnson form in the usual ultrasound range, say 500 kHz–5 MHz and then is cut off. We suggest assuming something which is asymptotically equivalent to the Johnson $\hat{b}(\omega)$. To this end we choose for the high frequency limit of the Johnson–Koplik–Dashen model

$$\hat{b}_\epsilon(\omega) = 2\frac{\beta a_\infty}{\Lambda}\sqrt{i\rho_f\eta\omega}e^{-\epsilon\omega}, \tag{2.7}$$

which has the inverse Fourier transform

$$b(t) = \frac{\sqrt{\pi i\rho_f\eta}\beta a_\infty}{\Lambda}(\epsilon - it)^{-\frac{3}{2}}. \tag{2.8}$$

The reformulated Biot–Johnson–Koplik–Dashen equations thereby are

$$\begin{aligned}
\mu\nabla^2\mathbf{u} + \nabla[(\lambda+\mu)e + Q\epsilon] &= \frac{\partial^2}{\partial t^2}(\rho_{11}\mathbf{u} + \rho_{12}\mathbf{U}) + \delta\int_0^t (\epsilon - i\tau)^{-\frac{3}{2}}\frac{\partial}{\partial\tau}(\mathbf{u}-\mathbf{U})(t-\tau)\, d\tau,\\
\nabla[Qe + R\epsilon] &= \frac{\partial^2}{\partial t^2}(\rho_{12}\mathbf{u} + \rho_{22}\mathbf{U}) - \delta\int_0^t (\epsilon - i\tau)^{-\frac{3}{2}}\frac{\partial}{\partial\tau}(\mathbf{u}-\mathbf{U})\, t-(\tau)\, d\tau,
\end{aligned} \tag{2.9}$$

where $\delta := \frac{\sqrt{\pi i\rho_f\eta}\beta a_\infty}{\Lambda}$ is a known coefficient and ϵ is a relaxation coefficient which is chosen to leave the ultrasonic range undisturbed.

The effective elastic, Biot constants $P := \lambda + 2\mu$, Q and R are related to β, bulk modulus of the pore fluid K_f, bulk modulus of the trabecular bone K_s, bulk modulus of the porous skeletal frame K_b and the shear modulus of the composite as well as the skeletal frame $N := \mu$:

$$\begin{aligned}
P &:= \frac{(1-\beta)\left(1-\beta-\frac{K_b}{K_s}\right) + \beta\frac{K_s}{K_f}K_b}{1-\beta-\frac{K_b}{K_s}+\beta\frac{K_s}{K_f}} + \frac{4}{3}N,\\
Q &:= \frac{\left(1-\beta-\frac{K_b}{K_s}\right)\beta K_s}{1-\beta-\frac{K_b}{K_s}+\beta\frac{K_s}{K_f}},\\
R &:= \frac{\beta^2 K_s}{1-\beta-\frac{K_b}{K_s}+\beta\frac{K_s}{K_f}}.
\end{aligned} \tag{2.10}$$

3. Dissipation of energy due to a viscous fluid

In order to add fluid–fluid dissipation of energy we note that generalized shear laws exhibit a stress term on the system of the form

$$D_{ij} := \varepsilon(\dot{\mathbf{U}})_{ij} := \frac{1}{2}\left(\frac{\partial \dot{U}_i}{\partial x_j} + \frac{\partial \dot{U}_j}{\partial x_i}\right), \qquad S_{ij} = 2\eta(\dot{\gamma})\varepsilon_{ij}, \quad \text{where } \dot{\gamma} = \sqrt{2\text{tr}(D^t D)}$$

and, where S_{ij} is the ij-component of the stress tensor.

There are two widely used shear-dependent viscosity laws in practice. The first is the power law, or Ostwald–de Waele model

$$\eta(\dot{\gamma}) := \eta_0 (\dot{\gamma})^{r-2}, \quad 1 < r < 2, \ \eta_0 > 0, \tag{3.11}$$

and the Carreau law, which takes into account that polymers show a finite nonzero constant Newtonian viscosity at very low shear rates [22,23]

$$\eta(\dot{\gamma}) := \eta_0 \left(1 + (\tilde{\lambda}\dot{\gamma})^2\right)^{\frac{r-2}{2}}, \quad 1 < r < 2. \tag{3.12}$$

In general, $\eta(\dot{\gamma})$ will be assumed to obey one of these laws; however, for purposes of exposition we will use the power law in the derivation below. Similar arguments may be used for the Carreau case.

For the case of a mechanical system where the forces are conservative the equations of motion may be written as the Euler–Lagrange equations for the Lagrangian $L := K - V$ as

$$\frac{d}{dt}\left[\frac{\partial(K-V)}{\partial \dot{q}_r}\right] = \frac{\partial(K-V)}{\partial q_r}, \tag{3.13}$$

where the q_r are generalized coordinates, the $\dot{q}_r$ the generalized velocities and K, V are the kinetic energy and potential energy of the system. If the system is not conservative we have instead

$$\frac{d}{dt}\left[\frac{\partial K}{\partial \dot{q}_r}\right] = \frac{\partial K}{\partial q_r} - F_r, \tag{3.14}$$

where F_r is the nonconservative force applied to the system. In either case [24] we have

$$\frac{dp_r}{dt} - \frac{\partial K}{\partial q_r} = \begin{cases} -\dfrac{\partial V}{\partial q_r}, & \text{conservative} \\ F_r, & \text{nonconservative,} \end{cases} \tag{3.15}$$

where $p_r = \frac{\partial K}{\partial \dot{q}_r}$ is the rth component of the generalized momentum $\mathbf{p}$.

In the Biot case we already have one nonconservative force (2.4); here we add another term, namely the fluid to fluid dissipation force

$$\mathbf{F}_{\text{fluid–fluid}} = 2\nabla \cdot \left[\eta(\dot{\gamma})\varepsilon(\dot{\mathbf{U}})\right], \tag{3.16}$$

whose jth component has the form

$$2\partial_k \left(\eta(\dot{\gamma})\varepsilon(\dot{U})_{jk}\right). \tag{3.17}$$

From (2.3) and (3.15), the Euler–Lagrange equations of motion, in the low frequency range, are

$$\begin{aligned}
&\frac{\partial \sigma_{xx}}{\partial x} + \frac{\partial \sigma_{xy}}{\partial y} + \frac{\partial \sigma_{xz}}{\partial z} = \frac{d}{dt}\left(\frac{\partial K}{\partial \dot{u}_x}\right) + b\left(\dot{u}_x - \dot{U}_x\right), \\
&\frac{\partial \sigma_{xy}}{\partial x} + \frac{\partial \sigma_{yy}}{\partial y} + \frac{\partial \sigma_{yz}}{\partial z} = \frac{d}{dt}\left(\frac{\partial K}{\partial \dot{u}_y}\right) + b\left(\dot{u}_y - \dot{U}_y\right), \\
&\frac{\partial \sigma_{xz}}{\partial x} + \frac{\partial \sigma_{yz}}{\partial y} + \frac{\partial \sigma_{zz}}{\partial z} = \frac{d}{dt}\left(\frac{\partial K}{\partial \dot{u}_z}\right) + b\left(\dot{u}_x - \dot{U}_z\right), \\
&\frac{\partial \sigma}{\partial x} = \frac{d}{dt}\left(\frac{\partial K}{\partial \dot{U}_x}\right) - 2\partial_k\left(\eta(\dot{\gamma})\varepsilon(\dot{U})_{1k}\right) - b\left(\dot{u}_x - \dot{U}_x\right), \\
&\frac{\partial \sigma}{\partial y} = \frac{d}{dt}\left(\frac{\partial K}{\partial \dot{U}_y}\right) - 2\partial_k\left(\eta(\dot{\gamma})\varepsilon(\dot{U})_{2k}\right) - b\left(\dot{u}_y - \dot{U}_y\right), \\
&\frac{\partial \sigma}{\partial z} = \frac{d}{dt}\left(\frac{\partial K}{\partial \dot{U}_z}\right) - 2\partial_k\left(\eta(\dot{\gamma})\varepsilon(\dot{U})_{3k}\right) - b\left(\dot{u}_z - \dot{U}_z\right);
\end{aligned}$$

whereas, in the high frequency case we replace the fluid–solid interaction with the convolution integral form. Using the constitutive equations for the elastic material in the Euler–Lagrange equations yields the equations of motion [25,24]

$$\mu\nabla^2\mathbf{u} + \nabla[(\lambda+\mu)e + Q\epsilon = \frac{\partial^2}{\partial t^2}(\rho_{11}\mathbf{u} + \rho_{12}\mathbf{U}) + \int_0^t b(t-\tau)\frac{\partial}{\partial\tau}(\mathbf{u}-\mathbf{U})(\tau)\,d\tau,$$
$$\nabla\left[Qe + R\epsilon\right] + 2\nabla\cdot\left[\eta(\dot\gamma)\varepsilon(\dot{\mathbf{U}})\right] = \frac{\partial^2}{\partial t^2}(\rho_{12}\mathbf{u} + \rho_{22}\mathbf{U}) - \int_0^t b(t-\tau)\frac{\partial}{\partial\tau}(\mathbf{u}-\mathbf{U})(\tau)\,d\tau.$$

4. Quasi-time harmonic models

If the displacements take the form $\mathbf{u}(\mathbf{x})e^{-i\omega t}$, $\mathbf{U}(\mathbf{x})e^{-i\omega t}$, then

$$\dot\gamma = \sqrt{2\omega^2\varepsilon(U)_{ij}\overline{\varepsilon(U)_{ij}}} =: \omega E \tag{4.18}$$

where $E := \sqrt{2\varepsilon(U)_{ij}\overline{\varepsilon(U)}_{ij}}$.

After cancelation of the factor $e^{-i\omega t}$ the equations with a dissipation kernel $b(t)$ become

$$\mu\nabla^2\mathbf{u} + \nabla\left[(\lambda+\mu)e + Q\epsilon\right] = -\omega^2\left(\rho_{11}\mathbf{u} + \rho_{12}\mathbf{U}\right) - i\omega\left(\mathbf{u}-\mathbf{U}\right)(\mathbf{x})\int_0^t b(\tau)e^{-i}\omega\tau\,d\tau \tag{4.19}$$

$$\nabla\left[Qe + R\epsilon\right] - 2i\omega\nabla\cdot\left[\eta(\omega E)\varepsilon(U)\right] = -\omega^2(\rho_{12}\mathbf{u} + \rho_{22}\mathbf{U}) + i\omega\left(\mathbf{u}-\mathbf{U}\right)(\mathbf{x})\int_0^t b(\tau)e^{-i}\omega\tau\,d\tau. \tag{4.20}$$

Note that in (4.20) one needs to use

$$\nabla\eta(\dot\gamma) = \omega\eta'(\omega E)\nabla E.$$

Now if we let $t\to\infty$ this becomes the steady-state, time harmonic case

$$\mu\nabla^2\mathbf{u} + \nabla\left[(\lambda+\mu)e + Q\epsilon\right] = -\omega^2\left(\rho_{11}\mathbf{u} + \rho_{12}\mathbf{U}\right) - i\omega\left(\mathbf{u}-\mathbf{U}\right)(\mathbf{x})\hat b(\omega), \tag{4.21}$$

$$\nabla\left[Qe + R\epsilon\right] - 2i\omega\nabla\cdot\left[\eta(\omega E)\varepsilon(U)\right] = -\omega^2(\rho_{12}\mathbf{u} + \rho_{22}\mathbf{U}) + i\omega\left(\mathbf{u}-\mathbf{U}\right)(\mathbf{x})\hat b(\omega). \tag{4.22}$$

In the linear Biot model, without a shear-thinning fluid, taking the Fourier transform of the equations eliminates all dependency on time. We are unable to do this in the nonlinear case; however, we may view the time independent case as a large time form of the system. The one-dimensional version of the quasi-time harmonic Biot–Johnson [16] equations with a power-law, shear-thinning interstitial fluid become

$$-\omega^2\left[\tilde\rho_{11}(\omega)u + \tilde\rho_{12}(\omega)U\right] = P\frac{d^2u}{dx^2} + Q\frac{d^2U}{dx^2},$$
$$-\omega^2\left[\tilde\rho_{12}(\omega)u + \tilde\rho_{22}(\omega)U\right] = Q\frac{d^2u}{dx^2} + R\frac{d^2U}{dx^2} - i2^{r/2}\omega^{r-1}\eta_0\frac{d}{dx}\left(\left|\frac{dU}{dx}\right|^{r-2}\frac{dU}{dx}\right), \tag{4.23}$$

with the pseudo masses defined below

$$\tilde\rho_{11}(\omega) := \rho_{11} + \frac{2\beta\alpha_\infty}{\Lambda}\left(\frac{\rho_f\eta}{i\omega}\right)^{1/2}, \tag{4.24}$$

$$\tilde\rho_{12}(\omega) := \rho_{12} - \frac{2\beta\alpha_\infty}{\Lambda}\left(\frac{\rho_f\eta}{i\omega}\right)^{1/2}, \tag{4.25}$$

$$\tilde\rho_{22}(\omega) := \rho_{22} + \frac{2\beta\alpha_\infty}{\Lambda}\left(\frac{\rho_f\eta}{i\omega}\right)^{1/2}, \tag{4.26}$$

where ρ_{11}, ρ_{12}, ρ_{22} are the mass coupling terms in the Biot model defined in terms of solid density ρ_s, pore fluid density ρ_f, β, α_∞ and ω, namely

$$\rho_{12} := -\beta\rho_f(\alpha_\infty - 1), \qquad \rho_{22} := \beta\rho_f\alpha_\infty,$$
$$\rho_{11} := (1-\beta)\rho_s + \beta\rho_f(\alpha_\infty - 1). \tag{4.27}$$

5. One-dimensional models

5.1. Boundary conditions

The one-dimensional problem for the linear Biot model has been studied in detail. We shall use this information to help with the strain-thinning case. We assume that a segment of cancellous bone occupies the interval $[0, L]$ in an infinite water tank and that it is sonified by a source placed at the point $x_s < 0$. The one-dimensional version of the Biot equations with a shear-thinning interstitial fluid becomes in the quasi-time harmonic case [26]

$$\begin{aligned}
&-\omega^2\left[\tilde{\rho}_{11}(\omega)\hat{u} + \tilde{\rho}_{12}(\omega)\hat{U}\right] = P\frac{d^2\hat{u}}{dx^2} + Q\frac{d^2\hat{U}}{dx^2},\\
&-\omega^2\left[\tilde{\rho}_{12}(\omega)\hat{u}^s + \tilde{\rho}_{22}(\omega)\hat{U}\right] = Q\frac{d^2\hat{u}}{dx^2} + R\frac{d^2\hat{U}}{dx^2} - 2i\omega\frac{d}{dx}\left[\eta\,(\omega E)\,\frac{d\hat{U}}{dx}\right],
\end{aligned} \tag{5.28}$$

where the pseudo masses were defined previously. In the water tank, i.e. $(-\infty, 0) \cup (L, +\infty)$ the Fourier-transformed, acoustic waves satisfy the one-dimensional Helmholtz equation

$$\frac{\partial^2\hat{p}_0}{\partial x^2} + \frac{\omega^2}{c_0^2}\hat{p}_0 = -\hat{f}(\omega)\delta(x - x_s), \quad -\infty < x < 0. \tag{5.29}$$

This solution in the water is a fundamental, singular solution and has the form

$$\begin{aligned}
&\hat{p}_0 = C_1 e^{i\omega x/c_0}, \quad -\infty < x < x_s,\\
&\hat{p}_0 = C_2 e^{i\omega x/c_0} + C_3 e^{-i\omega x/c_0}, \quad x_s < x < 0,\\
&\hat{p}_0 = C_4 e^{-i\omega x/c_0}, \quad L < x < +\infty.
\end{aligned} \tag{5.30}$$

Here the coefficients C_1, C_2, C_3, C_4 need to be determined. In the linear case we are able to give a similar expansion for the displacements u, U in the cancellous region and determine all of the coefficients by imposing Biot transition conditions at the interfaces between bone and water. In the nonlinear case the problem is made more difficult as an analytical formula for the displacements is not available in the segment $[0, L]$ and we must use numerical methods. We mention, however that only two of the above three coefficients is independent as $p_0(x)$ is a Green's function and is continuous at x_s and whose derivative has a jump discontinuity. This leads to

$$\begin{aligned}
C_2 &= C_1 + \frac{ic_0\hat{f}(\omega)}{2\omega}e^{-\frac{i\omega x_S}{c_0}},\\
C_3 &= -\frac{ic_0\hat{f}(\omega)}{2\omega}e^{-\frac{i\omega x_S}{c_0}}.
\end{aligned}$$

The one-dimensional Biot transmission conditions at $x = 0$ are

$$\begin{aligned}
&\hat{u}^w(0^-) = \beta\hat{U}^b(0^+) + (1-\beta)\hat{u}^b u(0^+),\\
&p(0^-) = (\lambda + 2\mu + Q)\frac{\partial\hat{u}^b}{\partial x}(0^+) + (R+Q)\frac{\partial\hat{U}^b}{\partial x}(0^+),\\
&p(0^-) = \frac{1}{\beta}\left[Q\frac{\partial\hat{u}^b}{\partial x}(0^+) + R\frac{\partial\hat{U}^b}{\partial x}(0^+)\right],
\end{aligned} \tag{5.31}$$

and at $x = L$

$$\begin{aligned}
&\hat{u}^w(L^+) = \beta\hat{U}^b(L^-) + (1-\beta)\hat{u}^b(L^-),\\
&p(L^+) = (\lambda + 2\mu + Q)\frac{\partial\hat{u}^b}{\partial x}(L^-) + (R+Q)\frac{\partial\hat{U}^b}{\partial x}(L^-),\\
&p(L^+) = \frac{1}{\beta}\left[Q\frac{\partial\hat{u}^b}{\partial x}(L^-) + R\frac{\partial\hat{U}^b}{\partial x}(L^-)\right].
\end{aligned} \tag{5.32}$$

Using $U^w = \frac{1}{\rho^w\omega^2}\frac{\partial p}{\partial x}$ and the analytical expressions for $p(x)$ in the water these become at $x = 0$

$$\frac{i}{\rho^w c_0\omega}\left[C_1 + \frac{ic_0\hat{f}(\omega)}{\omega}\cos(\omega x_s)\right] = \beta\hat{U}^b(0^+) + (1-\beta)\hat{u}^b(0^+),$$

$$\left[C_1 + \frac{c_0\hat{f}}{\omega}\sin\left(\frac{\omega x_s}{c_0}\right)\right] = (\lambda + 2\mu + Q)\frac{\partial \hat{u}^b}{\partial x}(0^+) + (R+Q)\frac{\partial \hat{U}^b}{\partial x}(0^+),$$

$$\left[C_1 + \frac{c_0\hat{f}}{\omega}\sin\left(\frac{\omega x_s}{c_0}\right)\right] = \frac{1}{\beta}\left[Q\frac{\partial \hat{u}^b}{\partial x}(0^+) + R\frac{\partial \hat{U}^b}{\partial x}(0^+)\right]. \tag{5.33}$$

At $x = L$ we match the Biot transmission conditions at $x = L^-$ using the expression the water pressure at $x = L^+$.

$$\frac{-i}{c_0\omega}C_4 e^{-iL\omega/c_0} = \beta\hat{U}^b(L^-) + (1-\beta)\hat{u}^b(L^-),$$

$$C_4 e^{-i\omega L/c_0} = (\lambda + 2\mu + Q)\frac{\partial \hat{u}^b}{\partial x}(L^-) + (R+Q)\frac{\partial \hat{U}^b}{\partial x}(L^-),$$

$$C_4 e^{-i\omega L/c_0} = \frac{1}{\beta}\left[Q\frac{\partial \hat{u}^b}{\partial x}(L^-) + R\frac{\partial \hat{U}^b}{\partial x}(L^-)\right]. \tag{5.34}$$

We may now eliminate C_4 from these three conditions. Since we do not have an analytical expression for the solution in the bone region we use a numerical approach and choose a value of C_1 dictated by the solution to the linear problem and use this to begin an iteration process. If we know C_1, then the left-hand side of Eqs. (5.31) are known, and this leads to an overdetermined system. However, we may proceed to solve the problem numerically in $[0, L]$ using just the second and third conditions of (5.31) and then picking $\hat{u}^b(0)$ and $\hat{U}^b(0)$ satisfy the third condition of (5.33). Using a shooting method we check these against (5.34) and adjust C_1 and the choice of $\hat{u}^b(0)$ and $\hat{U}^b(0)$.

5.2. Numerical results

To illustrate the performance of our models, we perform numerical simulations and restrict ourselves to the one-dimensional Carreau model given by the Biot equations with a shear-thinning interstitial fluid in the quasi-time harmonic case [26]

$$-\omega^2\left[\tilde{\rho}_{11}(\omega)\hat{u} + \tilde{\rho}_{12}(\omega)\hat{U}\right] = P\frac{d^2\hat{u}}{dx^2} + Q\frac{d^2\hat{U}}{dx^2},$$

$$-\omega^2\left[\tilde{\rho}_{12}(\omega)\hat{u} + \tilde{\rho}_{22}(\omega)\hat{U}\right] = Q\frac{d^2\hat{u}}{dx^2} + R\frac{d^2\hat{U}}{dx^2} - 2i\omega\frac{d}{dx}\left[\eta\,(\omega E)\,\frac{d\hat{U}}{dx}\right], \tag{5.35}$$

where

$$\eta(\omega E) = \eta_0\left(1 + 2\tilde{\lambda}^2\omega^2\left|\frac{d\hat{U}}{dx}\right|^2\right)^{\frac{r-2}{2}}, \tag{5.36}$$

which is used for the value of η in the expressions of $\tilde{\rho}_{11}$, $\tilde{\rho}_{12}$ and $\tilde{\rho}_{22}$ in (4.24)–(4.26).

In order to perform numerical simulations, we first non-dimensionalize the equations. For this purpose, we introduce a characteristic length scale c_0/ω, a characteristic timescale $1/\omega$ and the saturating fluid density, ρ_f; here c_0 denotes the speed of sound in water.

The non-dimensionalized equations are then solved numerically using a second-order finite difference scheme: the second-order derivatives in the bulk equations (5.35) are discretized with a second-order central difference formula, while the first-order derivatives in the transmission conditions (5.33) at $x = 0$ (resp. (5.34) at $x = L$) are discretized with a second-order forward (resp. backward) difference formula. The resulting discretized equations form a nonlinear algebraic system for the unknowns $(\hat{u}, \hat{U}, C_1, C_4)$, which is solved iteratively using the routine *fsolve* in MATLAB. The initial guess is provided by the linear solution of (5.35) (corresponding to $r = 2$ or $\tilde{\lambda} = 0$), which is obtained directly by Gaussian elimination. This is the case of zero shear thinning.

The Biot–Johnson model has built-in dissipation of both the fluid and solid phases; however, the fluid in the original Biot–Johnson case is assumed to be inviscid. In the modified model, we have added a nonlinear fluid–fluid viscosity term that represents shear thinning. The nonlinear solution of (5.35) thus quantifies the relative importance of shear thinning in the Biot–Johnson model.

The physical parameters that we used are: $\beta = 0.9$, $\alpha_\infty = 1.13$, $\Lambda = 8\,\mu\text{m}$, $\rho_f = 1000\,\text{kg m}^{-3}$, $\rho_f = 1990\,\text{kg m}^{-3}$, $K_f = 2.4$ GPa, $\nu_s = 0.35$, $E_s = 10$ GPa, $\nu_b = 0.25$ and $E_b = 4.16$ GPa, following [27]. We chose a bone thickness $L = 35.3$ mm, $c = 1480\,\text{m s}^{-1}$, and $\sqrt{2}\tilde{\lambda} = 1$ s which is a typical value for blood according to [28], The source was located at $x_s = -2L/15$ with amplitude $\hat{f} = \rho_f c_0\omega^2$ and frequency $\omega = 2\pi$ MHz in the ultrasonic range. This implies that the coefficient $\tilde{\lambda}^2\omega^2$ in (5.36) is very large, which is similar to the power-law model.

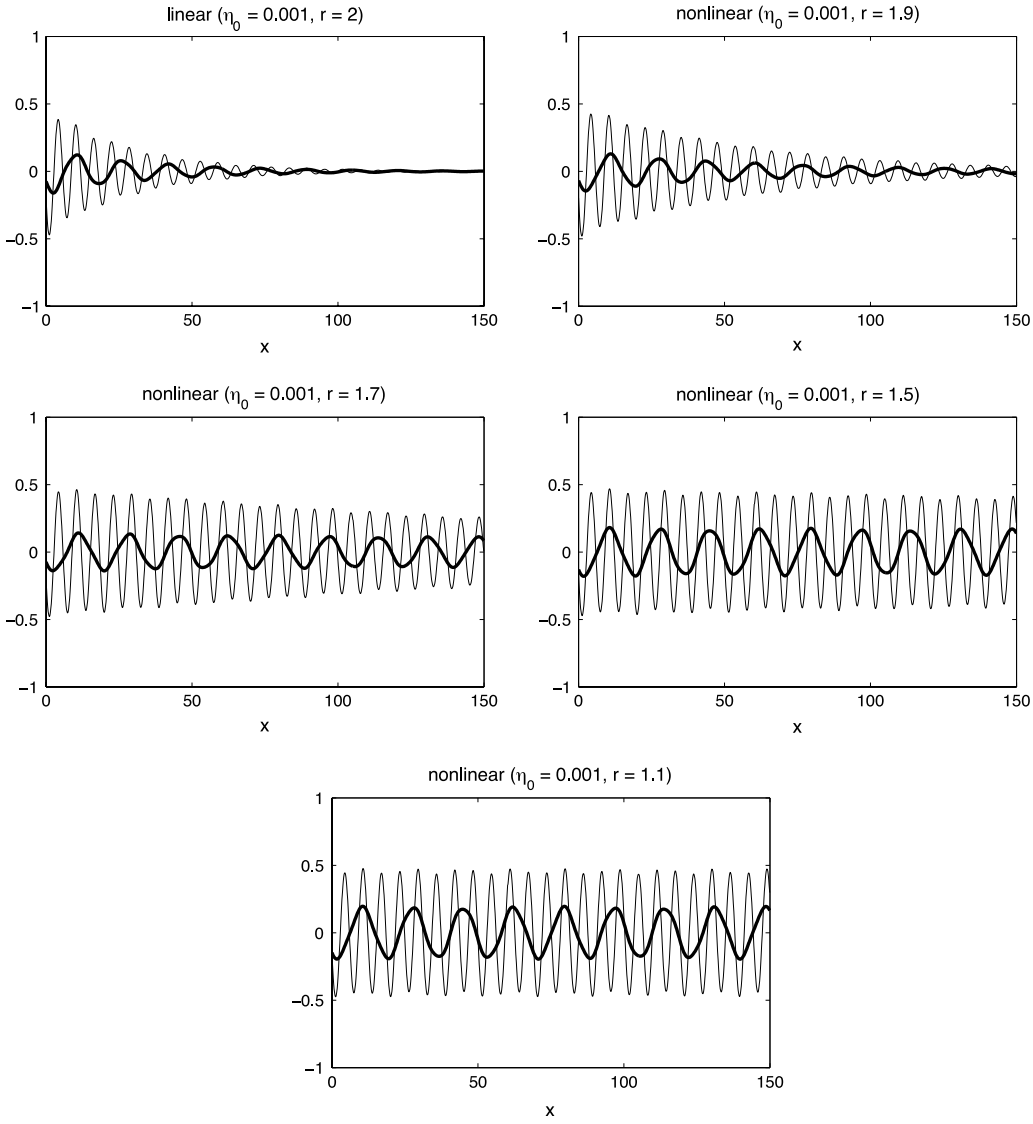

Fig. 1. Real parts of $\hat{u}$ (thick solid line) and $\hat{U}$ (thin solid line) for $r = 2, 1.9, 1.7, 1.5$ and 1.1. The frequency is $\omega = 2\pi$ MHz and the viscosity is $\eta_0 = 10^{-3}$ kg m^{-1} s^{-1} (water).

Figs. 1 and 2 show the real part of the displacements $(\hat{u}, \hat{U})$ for various values of η_0 and r. The smaller r (i.e. the closer to unity), the higher the nonlinearity while the smaller the effective viscosity η as compared to η_0, because $1 < r < 2$ in (5.36). We considered $\eta_0 = 10^{-3}$ kg m^{-1} s^{-1} which is a typical viscosity for water, and $\eta_0 = 10^{-1}$ kg m^{-1} s^{-1} a typical value for blood–marrow. The x-axis was partitioned into 1000 subintervals over $[0, L]$. This spatial resolution was found to be a good compromise between accuracy and computational cost.

Clearly, the nonlinearity due to shear thinning affects the fluid and solid displacements as compared to the linear case. In the situation of smaller viscosity ($\eta_0 = 10^{-3}$ kg m^{-1} s^{-1}) which is typically characterized by fluid displacements more oscillating than solid displacements (Fig. 1), Johnson's dissipative effect is evident for $r = 2$. As r decreases, the high nonlinearity weakens the effective viscosity so that the signal tends to become uniform across the bone thickness, meaning that both $\hat{u}$ and $\hat{U}$ tend to exhibit constant amplitudes. The only effect reminiscent of Johnson's dissipation is a phase shift between $\hat{u}$ and $\hat{U}$.

In the situation of larger viscosity ($\eta_0 = 10^{-1}$ kg m^{-1} s^{-1}), the fluid–solid system typically behaves like a single material. Therefore $\hat{u}$ and $\hat{U}$ tend to evolve in unison, as shown in Fig. 2 for $r \sim 2$. However, as r decreases, so does the effective viscosity and we observe phenomena similar to the case $\eta_0 = 10^{-3}$ kg m^{-1} s^{-1}.

To further assess the dissipative effects, Figs. 3 and 4 show the attenuation rate of $\hat{U}$ as a function of frequency $f = \omega/(2\pi)$, for $\eta_0 = 10^{-3}$ kg m^{-1} s^{-1} and $\eta_0 = 10^{-1}$ kg m^{-1} s^{-1} respectively. These results are obtained by fitting

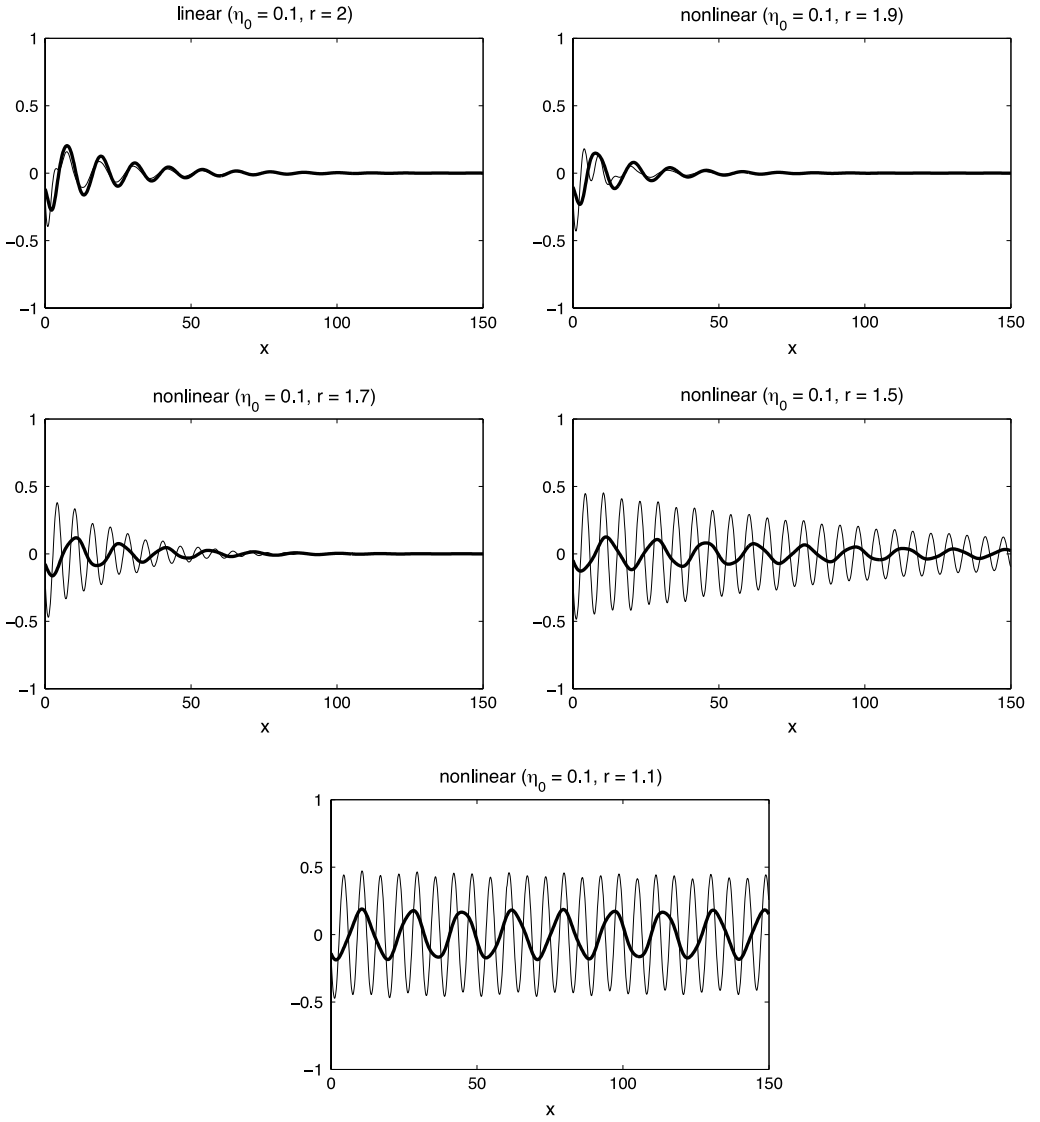

Fig. 2. Real parts of $\hat{u}$ (thick solid line) and $\hat{U}$ (thin solid line) for $r = 2, 1.9, 1.7, 1.5$ and 1.1. The frequency is $\omega = 2\pi$ MHz and the viscosity is $\eta_0 = 10^{-1}$ kg m^{-1} s^{-1} (blood–marrow).

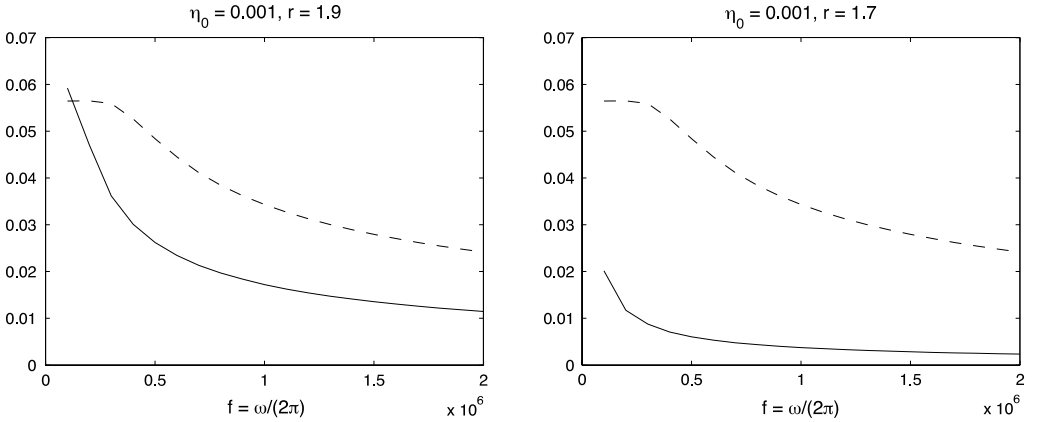

Fig. 3. Attenuation rate of $\hat{U}$ as a function of frequency for $\eta_0 = 10^{-3}$ kg m^{-1} s^{-1} with $r = 1.9$ (left) and $r = 1.7$ (right). The dashed line represents the linear model while the solid line represents the nonlinear model.

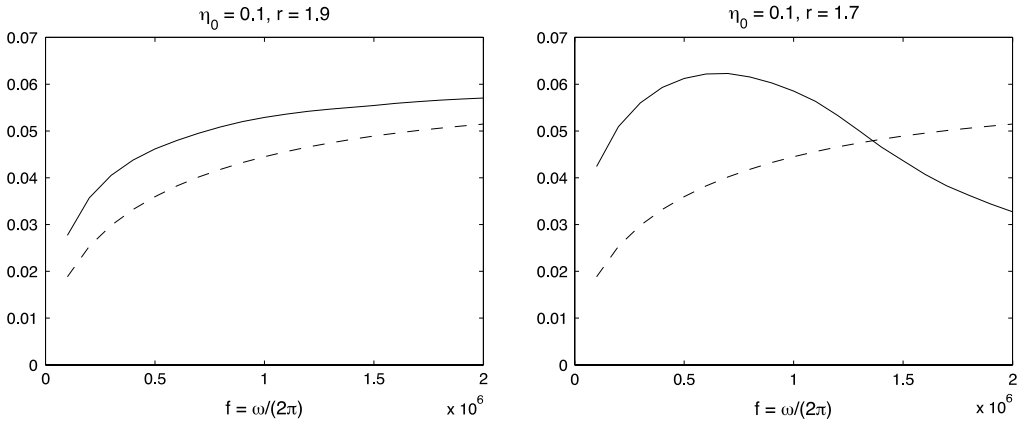

Fig. 4. Attenuation rate of $\hat{U}$ as a function of frequency for $\eta_0 = 10^{-1}$ kg m^{-1} s^{-1} with $r = 1.9$ (left) and $r = 1.7$ (right). The dashed line represents the linear model while the solid line represents the nonlinear model.

an exponential function of the form Be^{-Ax} to the envelope $|\hat{U}|$. The coefficient A estimated by linear regression then gives the attenuation rate. For $\eta_0 = 10^{-3}$ kg m^{-1} s^{-1}, we see that dissipation is stronger in the linear model than in the nonlinear one for most frequencies in the ultrasonic range considered. This discrepancy gets more pronounced with the nonlinearity (i.e. as r decreases). On the other hand, the situation is reversed for $\eta_0 = 10^{-1}$ kg m^{-1} s^{-1}. However, as the nonlinearity increases, dissipation weakens and accordingly the attenuation rate goes down for frequencies higher than $f \sim 0.7$ MHz. This is consistent with observations from Figs. 1 and 2 where the signal tends to become uniform as r decreases because of the weaker dissipation.

6. Conclusion

Another experiment involves computing the spectra of the phase velocity, $c(\omega)$ and that of the attenuation, $\alpha(\omega)$ where ω is the frequency of the sound wave. This apparent frequency-dependent attenuation is measured as $\alpha(\omega) = \ln \frac{|A^{\text{rec}}(\omega)|}{|A_0(\omega)|}$, where $A^{\text{rec}}(\omega)$ and $A(\omega)$ are the amplitude spectra of the received waveform that has been propagated through the medium and the initial amplitude respectively [29]. Using the above experimental set up, the spectral decomposition of the wave may be obtained by a simple computation [30]. Many investigations report attenuation depends linearly on frequency from 200 to 600 kHz and in the range of 600 kHz–1 MHz [31,3,32]. In this work attenuation $a(\omega)$ is a linear function of frequency, i.e. $a(\omega) = (\text{BUA})\omega + K$, with K being a constant. The term (BUA) is the gradient in dB/MHz evaluated by linear regression. Despite the fact that this technique, based on linear regression of the attenuation does not have any physical basis it is commonly accepted that the (BUA) gradient is relevant to the evaluation of osteoporosis [1]. Hofmeister [33] found that in the range 0.5–1 MHz BUA exhibited a significant correlation with the anterior–posterior (AP) and the medial–lateral (ML) directions but not in the superior–inferior (SI) orientations. A break point in the slopes was observed at about 1.0 MHz; whereas, other researchers observed one at about 400 kHz. Others observed measurable nonlinear attenuation at frequencies below 400 kHz for unfatted bone from human cadavers [34]. However, Chaffai [35] found that attenuation varied in terms of frequency roughly as $f^{1.1\pm0.3}$.

References

[1] Z.E.A. Fellah, J.Y. Chapelon, S. Berger, W. Lauriks, C. Depollier, Ultrasonic wave propagation in human cancellous bone: Application of Biot theory, J. Acoust. Soc. Am. 116 (2004) 61–73.
[2] F.J. Fry, J.E. Barger, Acoustical properties of the human skull, J. Acoust. Soc. Am. 63 (1978) 1576–1590.
[3] C.F. Njeh, C.M. Langton, The effect of cortical endplates on ultrasound velocity through the calcaneus: An in vitro study, Br. J. Radiol. 70 (1997) 504–510.
[4] S. Chaffai, F. Padilla, G. Berger, P. Languier, In vitro measurement of the frequency dependent attenuation in cancellous bone between 0.2 and 2 MHz, J. Acoust. Soc. Am. 108 (2000) 1281–1289.
[5] C.M. Langton, T.J. Haire, P.S. Ganney, C.A. Dobson, M.J. Fagan, G. Sisias, R. Phillips, Stochastically simulated assessment of anabolic treatment following varying degrees of cancellous bone resorption, Bone 27 (2000) 111–118.
[6] R.D. Stoll, Acoustic waves in saturated sediments, in: L. Hampton (Ed.), Physics of Sound in Marine Sediments, Plenum, New York, 1974.
[7] J.L. Williams, Prediction of some experimental results by Biot's theory, J. Acoust. Soc. Am. 91 (1992) 1106–1112.
[8] A. Hosokawa, T. Otani, Ultrasonic wave propagation in bovine cancellous bone, J. Acoust. Soc. Am. 101 (1997) 558–562.
[9] M.L. McKelvie, S.B. Palmer, The interaction of ultrasound with cancellous bone, Phys. Med. Biol. 10 (1991) 1331–1340.
[10] C. Picart, P. Carpentier, Human blood shear yield stress and its hematocrit dependence, J. Rheol. 42 (1) (1998).
[11] D.S. Sankara, K. Hemalathab, Non-Newtonian fluid flow model for blood flow through a catheterized artery steady flow, Appl. Math. Model. 31 (9) (2007) 1847–1864.
[12] G.B. Thurston, Viscoelasticity of human blood, Biophys. J. 12 (1972) 1205–1217.
[13] C.F. Njeh, C.M. Langton, The effect of cortical endplates on ultrasound velocity through the calcaneus: an in vitro study, Br. J. Radiol. 70 (1997) 504–510.
[14] C.M. Langton, C.F. Njeh, R. Hodgskinson, J.D. Curey, Prediction of mechanical properties of human cancellous by broadbeam ultrasonic attenuation, Bone 18 (1996) 495–503.

[15] P.E. Nicholson, M.L. Bouxsein, Bone marrow influences quaqntitative ultrasound measurements in human cancellous bone, Ultrasound Med. Biol. 28 (3) (2002) 369–375.
[16] D.L. Johnson, J. Koplik, R. Dashen, Theory of dynamic permeability and tortuousity in fluid-saturated porous media, J. Fluid Mech. 176 (1987) 379–402.
[17] A.E.H. Love, A Treatise on the Mathematical Theory of Elasticity, Dover, New York, 1944.
[18] M.A. Biot, Theory of propagation of elastic waves in a fluid-saturated porous solid. I. Lower frequency range, and II. Higher frequency range, J. Acoust. Soc. Am. 28 (2) (1956) 68–78 and 79–9.
[19] M.A. Biot, Mechanics of deformation and acoustic propagation in porous media, J. Appl. Phys. 33 (1962) 482–498.
[20] R.P. Gilbert, J.-P. Groby, Y. Liu, E. Ogam, A. Wirgin, Y.S. Xu, Computing porosity of cancellous bone using ultrasonic waves II: the muscle, cortical, cancellous bone system, Math. Comput. Modelling 50 (2009) 421–429.
[21] D.S. Jones, Generalized Functions, McGraw-Hill, New York, 1966.
[22] J.F. Agassant, P. Avenas, J. Sergent, P. Carreau, Polymer Processing, Principles and Modeling, Hasser, Munich, 1993.
[23] N. Phan-Thien, Understanding viscosity, in: Advanced Texts in Physics, Springer, Berlin, 2002.
[24] P.M. Morse, H. Feshbach, Methods of Theoretical Physics, Part 1, McGraw Hill, New York, 1953.
[25] R. Courant, D. Hilbert, Methods of Mathematical Physics: Volume 1, Interscience, New York, 1955.
[26] R.A. Shankaran, Numerical simulations of flow of shear-thinning fluids in corrugated channels, M.Sc. Thesis, Texas A & M University, 2007.
[27] N. Sebaa, Z.E.A. Fellah, M. Fellah, E. Ogam, A. Wirgin, F.G. Mitri, C. Depollier, W. Lauriks, Ultrasound characterization of human cancellous bone using the Biot theory: Inverse problem, J. Acoust. Soc. Am. 120 (2006) 1816–1824.
[28] J. Biasetti, H. Fazle, T.C. Gasser, Blood flow and coherent vortices in the normal and aneurysmatic aortas: a fluid dynamical approach to intra-luminal thrombus formation, J. R. Soc. Interface (2011), doi:10.1098/rsif.2011.0041.
[29] M. Sasso, G. Haiat, M. Talmant, P. Laugier, S. Naili, Singular value decomposition-based wave extraction in axial transmission: application to cortical bone ultrasonic characterization, IEEE Trans. Ultrason. Ferroelectr. Freq. Control 55 (2008) 1328.
[30] E. Ogam, Caractéisation ultrasonore et vibroacoustique de la santé mécanique des os humains, Ph.D. Thesis, Université de provence aix Marseille I, Marseille, France, 2007.
[31] C.M. Langton, S.B. Palmer, R.W. Porter, The measurement of broadband ultrasonic attenuation in cancellous bone, Eng. Med. 13 (1984) 89–91.
[32] C.F. Njeh, D.T. Hans, T. Fuerst, C.C. Gluer, H.K. Genant, Quantitative Ultrasound: Assessment of Osteoporosis and Bone Status, Martin Duniz, London, 1999, pp. 391–399.
[33] B.K. Hofmeister, S.A. Whitten, Y.J. Rao, Low megahertz ultrasonic properties of bovine cancellous bone, Bone 26 (9) (2000) 635–642.
[34] R. Srelitzki, J.A. Evans, On the measurement of the velocity of ultrasound in the calcis using short pulses, Eur. J. Ultrasound 4 (1996) 205–213.
[35] S. Chaffai, G. Berger, P. Langier, Frequency variation of ultrasonic attenuation coefficient of cancellous bone between 0.2 and 2.0 MHz, in: Proc. Ultrasonic Symp., 1998, pp. 1397–1400.